Received July 9, 2021; accepted July 31, 2021. Date of publication 3 August 2021; date of current version 11 August 2021.

Digital Object Identifier 10.1109/OJCOMS.2021.3102027

Performance Analysis of Hybrid Buffer-Aided Cooperative Protocol Based on Half-Duplex and Virtual Full-Duplex Relay Selections

GAN SRIRUTCHATABOON[1], JUN KOCHI[2], AND SHINYA SUGIURA[1] (Senior Member, IEEE)

[1]Institute of Industrial Science, The University of Tokyo, Tokyo 153-8505, Japan

[2]Department of Computer and Information Sciences, Tokyo University of Agriculture and Technology, Koganei 184-8588, Japan

CORRESPONDING AUTHOR: S. SUGIURA (e-mail: sugiura@iis.u-tokyo.ac.jp)

This work was supported in part by the Japan Society for the Promotion of Science (JSPS) KAKENHI under Grant 17H03259, and in part by the Japan Science and Technology Agency (JST) Precursory Research for Embryonic Science and Technology (PRESTO) under Grant JPMJPR1933. Part of this paper was submitted for presentation at IEEE GLOBECOM2021.

ABSTRACT This paper proposes a buffer-aided relay selection that is capable of exploiting both half-duplex and virtual full-duplex (VFD) transmissions in a hybrid manner. In the proposed scheme, we consider a two-hop cooperative network where each node is equipped with a single antenna, and no direct link between the source to the destination exists. The proposed scheme consists of five relay selection modes: two unicast modes, a broadcast mode, a cooperative beamforming mode, and a VFD mode. Owing to the broadcast mode, multiple relay nodes can seamlessly have a common packet; this mode is capable of solving the inter-relay interference problem imposed on the VFD mode. The proposed scheme's theoretical performance bounds on the throughput, the outage probability, and the delay are derived. It is demonstrated in our simulations that the proposed scheme attains higher performance in terms of a throughput and an outage probability than the conventional schemes while maintaining an acceptable average end-to-end delay profile.

INDEX TERMS Buffer, half-duplex, outage probability, relay selection, theoretical analysis, virtual full-duplex.

I. INTRODUCTION

THE CLASSIC relay-assisted cooperative communications [1], [2] were designed for exploiting the spatial diversity gain, hence increasing the capacity and coverage. In order to further increase the diversity gain in the conventional cooperative protocol, the class of buffer-aided relay selection was proposed [3]–[21] and leads to flexible transmission based on the quality of channel state information (CSI). In a two-hop buffer-aided relaying network, the max-max relay selection (MMRS) was developed [7], where source-to-relay (SR) and relay-to-destination (RD) links were activated alternately in each slot. The MMRS scheme can achieve a better average delay than the conventional counterparts that do not use the relay nodes' data buffers. In [8], the max-link (ML) scheme was conceived, where a single strongest link is activated for transmission in each slot, and a higher diversity order than the MMRS scheme counterpart is achieved. To avoid the detrimental overflow and empty states of buffers, the ML scheme was extended to the buffer-state-based (BSB) relay selection [17], [22]. Moreover, the concepts of generalized MMRS (G-MMRS) and generalized ML (G-ML) were developed [18]; these schemes exploit the broadcast nature of wireless channels, i.e., multiple SR links are simultaneously activated for allowing relay nodes to share a common packet. This increases the number of degrees of freedom, which improves performance of an outage probability and a delay profile in comparison to the conventional MMRS, ML, and BSB counterparts. The performance of the ML scheme was also investigated for a multi-hop wireless network in [23]. The idea of broadcast-based packet sharing is exploited in several other contexts,

such as in amplify-and-forward relaying [24], physical layer security [25], cognitive radio [26], and non-orthogonal multiple access (NOMA) [27], [28]. Furthermore, in [19], cooperative beamforming was incorporated into the G-ML protocol, where the outage probability is further reduced by the explicit benefit of the beamforming gain.

In full-duplex (FD) transmission [29], a transceiver simultaneously transmits and receives in the same resource slot and achieves a doubled transmission rate in comparison to that of traditional half-duplex (HD) transmission. While the FD transceiver suffers from strong self-interference, a number of techniques were developed for reducing such self-interference [30]–[32]. Also, cooperative communication with an FD relay node was proposed [33]. However, sufficient self-interference cancellation with a practical terminal cost is still an open issue. To combat this limitation, the concept of FD transmission is incorporated into buffer-aided relay selection with HD relay nodes, which is referred to as virtual full-duplex (VFD) [34]–[36]. In the VFD scheme, one relay node receives a packet from a source node while another relay node relay a different packet stored in its buffer to a destination node, thereby enabling FD transmission in a virtual manner without suffering from self-interference. However, in [34]–[36], the detrimental inter-relay interference (IRI) effects were ignored for simplicity. In [37], [38], the IRI effects specific to VFD were taken into consideration, allowing IRI to be canceled by multiple antenna processing at relay nodes. Additionally, the VFD scheme for multi-hop networks was investigated in [39]. Moreover, the algorithm of a low-latency for the successive opportunistic relaying (LoLA4SOR) was proposed in [40], which is capable of operating in both HD and VFD transmissions while maintaining the high diversity level and the low packet delay. In the LoLa4SOR scheme, if the VFD transmission fails to perform due to IRI effects, either the HD SR or HD RD link is selected for transmission. Furthermore, in [41], dirty paper coding (DPC) was exploited at the receiving relay to cancel the effects of IRI. However, DPC and decoding typically impose significantly high complexity, while the knowledge of inter-relay channel is needed at the source node. In [42], the maximum arrival rates of the FD scheme under the statistical delay constraints have been investigated. More recently, Nomikos *et al.* combined the concepts of FD and NOMA for buffer-aided opportunistic relay selection [43], [44], which increases the sum rate of the network.

Motivated by the above-mentioned backcloth, the novel contribution of this paper is that we propose buffer-aided relaying selection that relies on hybrid exploitation of VFD and HD transmission to increase an average throughput. The proposed scheme consists of five transmission modes: (1) an SR unicast mode, (2) an RD unicast mode, (3) an SR broadcasting mode, (4) an RD cooperative beamforming mode, and (5) a VFD mode for SR/RD transmission. Depending on CSI and buffer state information (BSI), the best mode is activated in each time slot. Specifically, since the VFD mode allows us to have a doubled rate compared to the other modes, the VFD mode is activated with a high priority. Since the relay nodes can share a packet with the aid of our broadcast mode, it is possible to carry out canceling of the effects of IRI imposed at a receiving relay node based on ideal successive interference cancellation (SIC). More specifically, under the assumption of common-packet sharing, the SIC of the proposed scheme is capable of perfectly eliminating interference.[1] The original idea of this paper was provided in our preliminary work [45], which, however, provide neither the mathematical analysis of the outage probability, the average packet delay, nor the throughput of the proposed scheme, while this paper does. Also, the comprehensive performance investigations and the validation between the analytical and numerical results are provided in this paper.

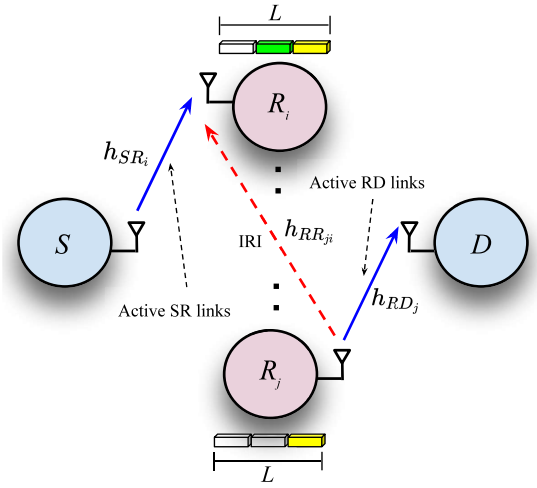

FIGURE 1. System model of the proposed scheme, consisting of a single source node, a single destination node, and multiple relay nodes with buffers.

The rest of this paper is structured as follows. In Section II, the system model is provided and in Section III, our relay selection algorithm is proposed. In Section IV, the theoretical bounds on an outage probability, a throughput, and a delay profile of the proposed scheme are derived. Then, we evaluate the performance of the proposed scheme in Section V. Finally, the present paper is concluded in Section VI.

II. SYSTEM MODEL

Fig. 1 depicts a relay network considered in this paper, which consists of a source node, multiple K relays nodes,

1. Note that similar to the proposed scheme, the NOMA-assisted buffer-aided relay selection scheme of [28] also relies on the activation of one out of multiple transmission and relaying modes. However, the NOMA and VFD modes are essentially different. In the uplink NOMA mode of [28], activated relay nodes simultaneously transmit their own packets to a destination node with appropriate power allocation. By contrast, in the VFD mode of the proposed scheme, each of the activated relay nodes are activated either as a receiving or a transmitting relay node, and then simultaneously transmit a buffered packet to a destination node or receive a packet from a source node. Hence, the proposed scheme elaborates on the cancellation of the detrimental IRI effects, unlike the NOMA-based scheme of [28].

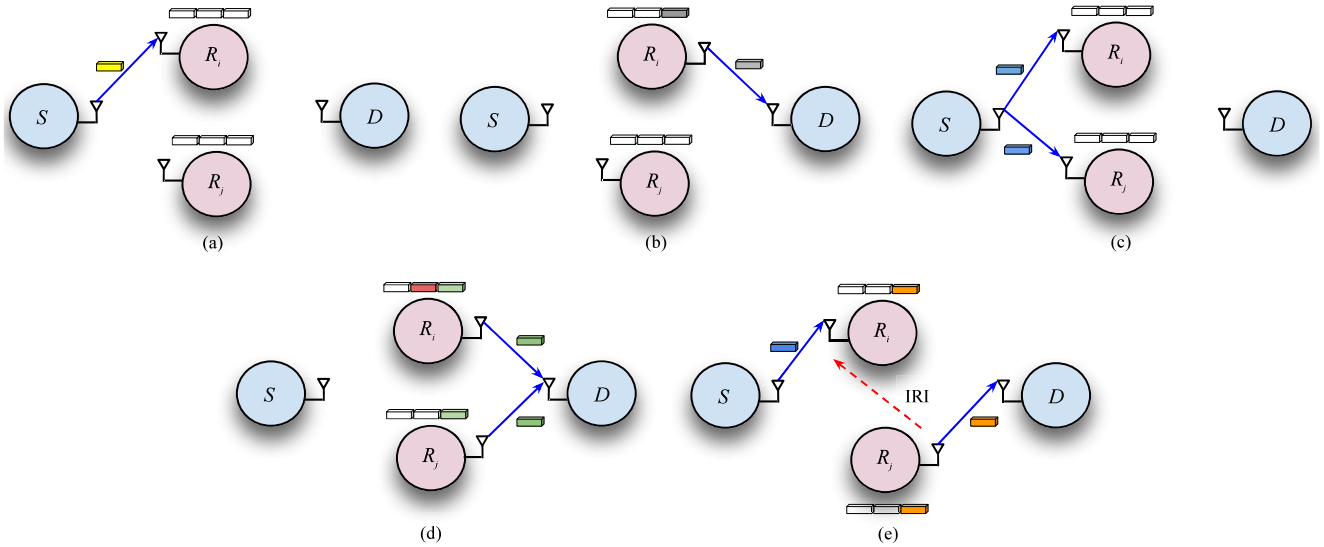

FIGURE 2. Five transmission modes in the proposed scheme; (a) SR unicast mode, (b) RD unicast mode, (c) SR broadcast mode, (d) RD cooperative beamforming mode, and (e) VFD mode for SR and RD transmissions.

and a destination node, where there is no direct source-to-destination (SD) link.[2] Each relay node is equipped with a data buffer with a size L. Also, we assume that each node has a single antenna element, operating under HD and decode-and-forward (DF) principles. The channel coefficients of the ith SR link, the relay-to-relay (RR) link between the ith and the jth relay nodes, and the jth RD link are denoted as h_{SR_i}, $h_{\mathrm{RR}_{ji}}$ and h_{RD_j}, respectively. All the links are assumed to follow independent frequency-flat Rayleigh block fading, where each channel coefficient remains unchanged over each time slot and it is generated as a random variable that obeys the zero-mean Gaussian distribution with a unit variance. Each node's transmission rate is fixed at r_0 bps/Hz.[3] After the destination node successfully decodes a packet, a one-bit acknowledge packet is broadcast from the destination node to the relay nodes with stable low-rate feedback links, and then the packet stored in the buffers is deleted.

Similar to previous studies on buffer-aided relay selection [7], [12], [18], we assume that the destination node acts as a central coordinator to collect and estimate CSI and BSI for each SR and RD link. The source node sends the pilot signal to the K relays, and each relay node then estimates the CSI based on the received pilot signal. After that, the estimated CSI and BSI are transmitted to the destination node. Finally, each relay node sends the pilot signal to the destination node for the estimation of each RD link's CSI. We assume that the central coordinator determines the transmission mode in each time slot based on the estimated CSI and BSI. However, when the channels vary slowly, the frequency of the CSI and BSI updates may be reduced to once every channel coherence time.[4]

In our protocol, the transmission is classified into five modes: 1) a unicast mode for SR transmission, 2) a unicast mode for RD transmission, 3) a broadcasting mode for SR transmission, 4) a cooperative beamforming mode for RD transmission, and 5) a VFD mode for SR and RD transmissions, which correspond to Figs. 2(a)–2(e), respectively. Similar to most previous buffer-aided relay selection schemes, in the proposed scheme, to activate an SR link, the buffer of the associated relay node has to have an empty slot. Similarly, to activate an RD link, the associated relay node has to have at least one packet in the buffer.

To expound a little further, it may be readily possible to include other transmission modes, such as the NOMA mode [27], [28], [48], the bidirectional mode [49], [50], and the underlay cognitive mode [26], into our scheme. However, our focus is on the introduction of the SIC-based VFD mode with the aid of packet sharing among the relay nodes.

A. UNICAST MODE FOR SR LINK

Fig. 2(a) illustrates the unicast mode for the selected SR link, where a packet is stored at the buffer of the selected relay node. The channel capacity of the ith SR link is given by

$$\mathcal{C}_{\mathrm{Uni}}^{\mathrm{SR}}(i) = \frac{1}{2}\log_2\left(1 + \left|h_{\mathrm{SR}_{(i)}}\right|^2 \gamma_{\mathrm{SR}}\right), \tag{1}$$

2. If there is a stable direct SD link, a two-hop relaying network does not have to be considered. Hence, in this paper, we focus our attention on the scenario of an unreliable SD link, such that an SD link is blocked or the source and destination nodes are apart far from each other.

3. The buffer-aided relay selection schemes are classified into fixed-rate and adaptive-rate ones. The adaptive-rate relay selection achieves high bandwidth efficiency, while the fixed-rate power-adaptive relay selection exhibits a higher power efficiency. More specifically, in fixed-rate relay selection, a transmit power that satisfies the activation criterion is set at each transmitting node. Hence, given a fixed transmission rate, the power consumption may be minimized as far as the transmission does not fall into outage, which corresponds to well-known quality-of-service (QoS) transmission.

4. When the channels change rapidly, or the CSI/BSI feedback errors exist, the achievable performance may deteriorate. To combat this limitation, several relay selection protocols with outdated CSI have been developed [46], [47].

where γ_{SR} denotes the average signal-to-noise ratio (SNR) of the SR links. If $\mathcal{C}_{\mathrm{Uni}}^{\mathrm{SR}_{(i)}} > r_0$ and the buffer of the ith relay node is not full, then the associated unicast from the source node to the ith relay node is successful.

B. UNICAST MODE FOR RD LINK

Fig. 2(b) shows the unicast mode for the selected RD link, similar to the unicast mode for SR transmission of Section II-A. The channel capacity of the jth RD link is given by

$$\mathcal{C}_{\mathrm{Uni}}^{\mathrm{RD}}(j) = \frac{1}{2}\log_2\Big(1 + |h_{\mathrm{RD}_{(j)}}|^2\gamma_{\mathrm{RD}}\Big), \tag{2}$$

where γ_{RD} is the average SNR of the RD links. If $\mathcal{C}_{\mathrm{Uni}}^{\mathrm{RD}_{(j)}} > r_0$ and if the buffer of the jth relay node is not empty, the corresponding unicast from the jth relay node to the destination node is successful.

C. BROADCAST MODE FOR SR LINKS

Fig. 2(c) shows the broadcast mode for SR links, where multiple SR links are activated simultaneously, which is possible without imposing an additional time slot owing to the broadcast nature of wireless channels. An information packet is transmitted from the source node to the relay nodes associated with the activated SR links. To distinguish the unicast mode and the broadcast mode, the case where only a single SR link is activated is defined as the unicast mode for SR transmission, rather than the broadcast mode.

Let us define the index set of the activated SR links as $\mathcal{T} \in \{1, \ldots, K\}$. Then, the broadcast mode is successful when all the buffers of the activated relay nodes are not full and all the capacities of the activated SR links are higher than r_0. More specifically, the ith SR link is included in the activated link set $\mathcal{T}$, if it satisfies:

$$\mathcal{C}_{\mathrm{Uni}}^{\mathrm{SR}}(i) \geq r_0. \tag{3}$$

Note that this broadcast mode plays an important role in the proposed scheme since the packet sharing among the relay nodes allows us to seamlessly carry out SIC in the cooperative beamforming and VFD modes, which is achieved without relying on the use of multiple antenna elements at the relay nodes.[5]

D. COOPERATIVE BEAMFORMING MODE FOR RD LINKS

Fig. 2(d) shows the cooperative beamforming mode for RD transmission, where a packet shared among a subset of the relay nodes is simultaneously transmitted from the selected relay nodes to the destination node in a coherent manner. The transmission weight at the jth relay node is set to $w_j = g_j^*/\|\mathbf{g}_c\|$, where we have $\mathbf{g}_c = [g_1, g_2, \ldots, g_K]^T$. The weights corresponding to the selected relay nodes are the same as the corresponding RD links, i.e., $g_j = h_{\mathrm{RD}_j}$, while those of the unselected relay nodes are set to zero.

The capacity of all RD links for the cooperative beamforming mode is given by

$$\mathcal{C}_{\mathrm{Beam}}^{\mathrm{RD}}(\mathbf{g}_c) = \frac{1}{2}\log_2\Big(1 + \|\mathbf{g}_c\|^2\gamma_{\mathrm{RD}}\Big). \tag{4}$$

Note that each cooperating relay node has to have the associated channel coefficients $\mathbf{g}_c$, which may be provided from the central coordinator. Furthermore, to carry out cooperative beamforming, the cooperating relay nodes need to be precisely synchronized.

E. VFD MODE FOR SR AND RD TRANSMISSIONS

All the above four modes (Sections II-A–II-D) operate under the HD principle, where either transmission or reception is done at the relay nodes in each time slot. By contrast, Fig. 2(e) shows the VFD mode, where a single receiving relay node receives a packet from the source node, while another single transmitting relay node transmits a packet in the buffer to the destination node simultaneously. Let us assume that the ith and the jth relay nodes as the receiving and transmitting relay nodes, respectively. Then, the signal received at the receiving relay node and that received at the destination node are given by

$$y_{\mathcal{R}}(i) = h_{\mathrm{SR}_i}x_{\mathcal{S}} + h_{\mathrm{RR}_{ji}}x_j + n_i \tag{5}$$

$$y_{\mathcal{D}}(j) = h_{\mathrm{RD}_j}x_j + n_{\mathcal{D}}, \tag{6}$$

where $x_{\mathcal{S}}$ and x_j denote packets transmitted from the source node and the jth relay node, respectively. Also, n_i and $n_{\mathcal{D}}$ are the associated AWGNs.

Here, since we assume that a packet transmitted from the jth relay node is shared between the ith and jth relay nodes, the ith relay can calculate $h_{\mathrm{RR}_{ji}}x_j$ with the aid of the channel estimation of $h_{\mathrm{RR}_{ji}}$. Then, the received signal (5) is modified to

$$\begin{aligned}\tilde{y}_{\mathcal{R}}(i) &= y_{\mathcal{R}}(i) - h_{\mathrm{RR}_{ji}}x_j \\ &= h_{\mathrm{SR}_i}x_{\mathcal{S}} + n_i.\end{aligned} \tag{7}$$

The channel capacities corresponding to (7) and (6) are given by

$$\mathcal{C}_{\mathrm{VFD}}^{\mathrm{SR}}(i) = \frac{1}{2}\log_2\Big(1 + |h_{\mathrm{SR}_i}|^2\gamma_{\mathrm{SR}}\Big) \tag{8}$$

$$\mathcal{C}_{\mathrm{VFD}}^{\mathrm{RD}}(j) = \frac{1}{2}\log_2(1 + |h_{\mathrm{RD}_j}|^2\gamma_{\mathrm{RD}}), \tag{9}$$

respectively. In order to activate the VFD mode, the receiving and transmitting relay nodes have to have a common packet in their buffers; this packet is used for eliminating IRI at the receiving relay node with SIC. Hence, we have the relationship $\mathcal{C}_{\mathrm{VFD}}^{\mathrm{SR}}(i) = \mathcal{C}_{\mathrm{Uni}}^{\mathrm{SR}}(i)$. The VFD mode is not

5. While employing multiple antennas at relay nodes enables the IRI cancellation, there are drawbacks. First, the antenna's degree of freedom is consumed to cancel the IRI effects. This implies that the proposed scheme is capable of exploiting such an unused antenna's degree of freedom for increasing beamforming or multiplexing gain when multiple antennas are used at relay nodes. Second, in the recent Internet of Things (IoT) and device-to-device (D2D) communications, all the nodes in the network are not necessarily equipped with multiple antenna elements.

in outage when both of capacities $\mathcal{C}_{\mathrm{VFD}}^{\mathrm{SR}}(i)$ and $\mathcal{C}_{\mathrm{VFD}}^{\mathrm{RD}}(j)$ are higher than the target rate r_0, i.e.,

$$\min\left\{\mathcal{C}_{\mathrm{VFD}}^{\mathrm{SR}}(i), \mathcal{C}_{\mathrm{VFD}}^{\mathrm{RD}}(j)\right\} \geq r_0. \tag{10}$$

Note that according to (10), we assume that when the VFD mode is in an outage, both the SR and RD transmissions fail, for simplicity. However, it may be possible that either of the SR and RD transmissions may be successful, even in the outage event of the VFD mode. To take into account this effect, the other definition may be employed. (See [50] for detail.)

In the VFD mode, two parallel SR and RD links are activated, and the total transmission rate is doubled compared to the other four modes. Hence, in our protocol, the VFD mode is activated as many times as possible, as shown in the following section. Furthermore, note that in SIC of (7), the receiving relay node has to have the RR channel $h_{\mathrm{RR}_{ji}}$. In our scheme, the relay nodes periodically transmit pilot symbols to the central coordinator, and hence the receiving relay node can overhear the pilot transmission from the transmitting relay node to estimate the associated RR channel coefficient.

III. PROPOSED ALGORITHM

Our relay selection algorithm is designed for operating using the VFD transmission as often as possible in order to increase the average throughput. In order to activate the VFD mode, the following constraints have to be satisfied.

- (C1) The receiving and the transmitting relay nodes (i, j) are different, i.e., $i \neq j$.
- (C2) The receiving and the transmitting relay nodes have a common packet in their buffers.
- (C3) The SR and RD links associated with the receiving and transmitting relay nodes are not in outage, i.e., the inequality (10) is satisfied.

More specifically, (C1) constraints the selected receiving and transmitting relay nodes are different, similar to [35], [37], [38]. This is because, in this paper, we focus on VFD transmission rather than the full-duplex transmission suffered from self-interference. Also, (C2) imposes the constraint needed to operate SIC at the receiving relay node, based on a shared packet between the two relay nodes. Furthermore, (C3) is the condition needed for successful simultaneous SR and RD transmissions in our VFD mode.

If these three constraints (C1)–(C3) are not satisfied, instead of the VFD mode, one of the other four HD modes is activated based on the priorities of the available SR and RD links. Only when all the constraints (C1)–(C3) are satisfied the VFD mode is activated. Herein, we define $\Theta_{i,j}$ as the set of the SR and RD link pairs that satisfy (C1)–(C3).

A. CASE OF $\Theta_{i,j} \neq \emptyset$

Let us consider the case where the VFD mode is activated, i.e., $\Theta_{i,j} \neq \varnothing$. According to [35], we assume that the strongest link pair between SR and RD links is selected for the VFD transmission, which is given by

$$\left(\hat{i}, \hat{j}\right) = \underset{i,j \in \Theta_{i,j}}{\arg\max} \left\{\min\left(\mathcal{C}_{\mathrm{VFD}}^{\mathrm{SR}}(i), \mathcal{C}_{\mathrm{VFD}}^{\mathrm{RD}}(j)\right)\right\}, \tag{11}$$

where $\hat{i}$ and $\hat{j}$ are the indices of the selected receiving and transmitting relay nodes, respectively. The reason to select a strongest link pair is that the transmit power consumption is reduced as far as transmission does not fall into outage, which corresponds to fixed-rate power-adaptive transmission.

B. CASES OF $\Theta_{i,j} = \emptyset$

By contrast, when any of the constraints (C1)–(C3) is not satisfied, one of the four HD modes is selected based on the priorities of the available SR and RD links corresponding to BSI. Similar to [19], [25], [26], [28], let us introduce the target number of packets stored in the buffer of the kth relay node as ζ_k. More specifically, ζ_k provides the priority to the selection of RD link or SR link, depending on whether the number of packets stored at the relay nodes exceeds ζ_k or not. When ζ_k is higher than the number of packets stored at the relay node, an RD transmission mode tends to be activated. Otherwise, an SR transmission mode has the priority to be selected. The detailed function of this thresholding parameter is found in [19], [25], [26], [28]. The difference from the target number of packets is calculated by

$$\Delta_k = \Psi_k - \zeta_k, \quad k \in \{1, \ldots, K\}. \tag{12}$$

This gives us the priority of each of the available SR and RD links as follows.

- The priority of the ith SR link is set to high if $\Delta_k < 0$, where $k = i$.
- The priority of the jth RD link is set to high if $\Delta_k \geq 0$, where $k = j$.

Let us define the numbers of the SR and RD links with high priority as $q^{(i)}$ and $q^{(j)}$, respectively. Based on $q^{(i)}$ and $q^{(j)}$, we can select one of four modes as follows.

1) $q^{(i)} > q^{(j)}$

When $q^{(i)} > q^{(j)}$, one of the two SR modes, i.e., the unicast and broadcast modes, is activated. The broadcast mode is activated if multiple SR links are not in outage and if the buffers of the associated relay nodes are not full. Otherwise, the unicast mode is activated by selecting a single strongest SR link.

2) $q^{(i)} < q^{(j)}$

When $q^{(i)} < q^{(j)}$, one of the two RD modes, i.e., the unicast and the cooperative beamforming modes, is selected. If multiple RD links are not in outage and the buffers of the associated relay nodes are not empty, then the cooperative beamforming mode for RD transmission is activated. Otherwise, the unicast mode for RD transmission is activated by selecting a single strongest RD link.

Algorithm 1 The Summary of the Proposed Algorithm

Require: $\Theta_{i,j}$, $q^{(i)}$, $q^{(j)}$
if $\Theta_{i,j} \neq \varnothing$ **then**
  VFD mod is activated.
  $(R_{\hat{i}}, R_{\hat{j}}) = \arg\max_{i,j\in\Theta_{i,j}}\{\min(\mathcal{C}^{\mathrm{SR}}_{\mathrm{VFD}}(i), \mathcal{C}^{\mathrm{RD}}_{\mathrm{VFD}}(j))\}$
else
  if $q^{(i)} > q^{(j)}$ **then**
    if $q^{(i)} = 1$ **then**
      SR unicast mod is activated.
    else
      SR broadcast mode is activated.
    end if
  end if
  if $q^{(j)} > q^{(i)}$ **then**
    if $q^{(j)} = 1$ **then**
      RD unicast mod is activated.
    else
      RD beamforming mode is activated.
    end if
  end if
  if $q^{(i)} = q^{(j)}$ **then**
    If the strongest link is an SR link, one of the two SR modes is activated according to 1)
    If the strongest link is an RD link, one of the two RD modes is activated according to 2)
  end if
end if

3) $q^{(i)} = q^{(j)}$

For $q^{(i)} = q^{(j)}$, either the SR transmission mode (the unicast or the broadcast mode) or the RD transmission mode (the unicast or the cooperative beamforming mode) is selected. If the strongest link is an SR one, then one of the two SR modes is activated according to 1). Similarly, if the strongest link is the RD one, then one of the two RD modes is activated according to 2).

The proposed selection algorithm is summarized in Algorithm 1.

IV. THEORETICAL BOUNDS

In this section, we derive the theoretical bounds on the outage probability, the throughput, and the average delay. First, we formulate the probability of successful transmission for each mode under the assumption that specific link(s) are selected. Then, we provide the state transition matrix.

A. SUCCESSFUL TRANSMISSION PROBABILITY

1) UNICAST MODE FOR SR AND RD TRANSMISSION

According to [17] and [19], the probability that a single specific SR or RD link is not in an outage event is given respectively by

$$\mathrm{P}^{\mathrm{SR}}_{\mathrm{Single}} = \int_{\frac{\gamma_t}{\gamma_{\mathrm{SR}}}}^{\infty} e^{-x}\mathrm{d}x = e^{-\frac{\gamma_t}{\gamma_{\mathrm{SR}}}} \tag{13}$$

$$\mathrm{P}^{\mathrm{RD}}_{\mathrm{Single}} = \int_{\frac{\gamma_t}{\gamma_{\mathrm{RD}}}}^{\infty} e^{-x}\mathrm{d}x = e^{-\frac{\gamma_t}{\gamma_{\mathrm{RD}}}}, \tag{14}$$

where

$$\gamma_t = 2^{2r_0} - 1. \tag{15}$$

2) BROADCAST MODE FOR SR TRANSMISSION

In the broadcast mode, multiple SR links are simultaneously activated to deliver a packet to the associated relays. Here, we denote the number of activated SR links as Q_{SR}. From (13), the probability that specific Q_{SR} SR links are not in an outage event is given by

$$\mathrm{P}^{\mathrm{SR}}_{\mathrm{Mul}} = \left(\mathrm{P}^{\mathrm{SR}}_{\mathrm{Single}}\right)^{Q_{\mathrm{SR}}} \tag{16}$$

$$= e^{-\frac{Q_{\mathrm{SR}}\gamma_t}{\gamma_{\mathrm{SR}}}}. \tag{17}$$

3) COOPERATIVE BEAMFORMING MODE FOR RD TRANSMISSION

In the cooperative beamforming mode, multiple RD links are coherently activated to send a common packet to the destination node. According to [51], the probability distribution of a sum of independent exponential distributions is a gamma distribution, i.e.,

$$f(Q_{\mathrm{RD}}, \lambda) = \frac{\lambda^{Q_{\mathrm{RD}}}}{\Gamma(Q_{\mathrm{RD}})} x^{Q_{\mathrm{RD}}-1} e^{-\lambda x}, \tag{18}$$

where λ is the variance of the fading channels, Q_{RD} is the number of activated RD links, and

$$\Gamma(Q_{\mathrm{RD}}) = \int_0^{\infty} t^{Q_{\mathrm{RD}}-1} e^{-t}\mathrm{d}t. \tag{19}$$

For example, let us consider the case that $Q_{\mathrm{RD}} = 2$ specific RD links are selected for cooperative beamforming. Also, recall that we consider channel coefficients with unit variance, i.e., $\lambda = 1$. Then, from (18), the successful transmission probability for cooperative beamforming with the activations of $Q_{\mathrm{RD}} = 2$ specific RD links is given by

$$\mathrm{P}^{\mathrm{RD}}_{\mathrm{Coop}} = \int_{\frac{\gamma_t}{\gamma_{\mathrm{RD}}}}^{\infty} \frac{1}{\Gamma(2)} x e^{-x}\mathrm{d}x \tag{20}$$

$$= \int_{\frac{\gamma_t}{\gamma_{\mathrm{RD}}}}^{\infty} x e^{-x}\mathrm{d}x \tag{21}$$

$$= \left(1 + \frac{\gamma_t}{\gamma_{\mathrm{RD}}}\right) e^{-\frac{\gamma_t}{\gamma_{\mathrm{RD}}}}. \tag{22}$$

4) VFD MODE

In the VFD mode, SR and RD links are simultaneously activated, where we are assuming that the related relay nodes have a common packet in the buffers. Given that specific SR and RD links are activated, the associated successful transmission probability is calculated by

$$\mathrm{P}_{\mathrm{VFD}} = \mathrm{P}^{\mathrm{SR}}_{\mathrm{Single}} \cdot \mathrm{P}^{\mathrm{RD}}_{\mathrm{Single}}. \tag{23}$$

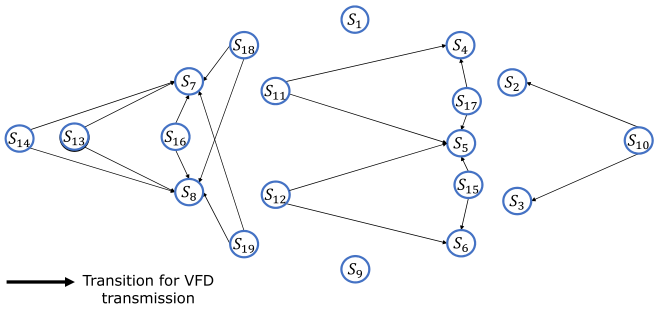

FIGURE 3. The proposed scheme's state diagram for the system parameters $(K, L) = (2, 2)$.

B. THEORETICAL OUTAGE PROBABILITY BOUND

Next, we derive the theoretical bound on the outage probability. Let us define a transition matrix as $\mathbf{A} \in \mathbb{R}^{N_{\text{state}} \times N_{\text{state}}}$, where the pth-row and qth-column entry A_{pq} represents the transition probability from state s_q to state s_p and N_{state} is the number of sets of all possible legitimate states. We denote S^{VFD} is the set of the states, which have the potential to perform the VFD mode in terms of buffer states. For example, the system with the parameters $(K, L) = (2, 2)$ has $N_{\text{state}} = 19$ legitimate states; these states are the same as those listed in [18, Table III]. The associated transition state diagram of the Markov chain model for the VFD mode is presented in Fig. 3, while the transitions for the four HD modes of our scheme are similar to those in the conventional G-ML scheme in [19].

We denote Ξ_q, Ξ_{pq}^{SR}, and Ξ_{pq}^{RD} by the sets of legitimate links, available SR links, and available RD links for state s_q. Furthermore, we consider the sets of available SR and RD links as $\Xi_{pq} = \Xi_{pq}^{\text{SR}} \cup \Xi_{pq}^{\text{RD}}$ for state s_q. Then, the transition probability from state s_q to state s_p is represented by

$$A_{pq} = \begin{cases} \mathrm{P}\left(\Xi_{pq}^{\text{SR}}\right) & \text{if } s_q \notin S^{\text{VFD}} \text{ and } q^{(i)} > q^{(j)} \\ \sum_{\Xi_{pq}^{\text{RD}} \subset \Xi_q} \mathrm{P}\left(\Xi_{pq}^{\text{RD}}\right) & \text{if } s_q \notin S^{\text{VFD}} \text{ and } q^{(i)} < q^{(j)} \\ \sum_{\Xi_{pq} \subset \Xi_q} \mathrm{P}\left(\Xi_{pq}\right) & \\ \times \mathrm{P}\left(s_q \to s_p | \Xi_{pq}\right) & \text{otherwise,} \end{cases} \tag{24}$$

where $\mathrm{P}(\Xi_{pq}) = \mathrm{P}(\Xi_{pq}^{\text{SR}}) \cdot \mathrm{P}(\Xi_{pq}^{\text{RD}})$. Moreover, $\Pr(\Xi_{pq}^{\text{SR}})$ and $\Pr(\Xi_{pq}^{\text{RD}})$ are the probabilities that a subset Ξ_{pq}^{SR} and a subset Ξ_{pq}^{RD} can successfully deliver a packet, which is expressed respectively, by

$$\mathrm{P}\left(\Xi_{pq}^{\text{SR}}\right) = \left(\mathrm{P}_{\text{Single}}^{\text{SR}}\right)^{Q_{\text{SR}}} \left(1 - \mathrm{P}_{\text{Single}}^{\text{SR}}\right)^{K - Q_{\text{SD}}} \tag{25}$$

$$\mathrm{P}\left(\Xi_{pq}^{\text{RD}}\right) = \left(\mathrm{P}_{\text{Single}}^{\text{RD}}\right)^{Q_{\text{RD}}} \left(1 - \mathrm{P}_{\text{Single}}^{\text{RD}}\right)^{K - Q_{\text{RD}}}. \tag{26}$$

Also, $\mathrm{P}(s_q \to s_p | \Xi_{pq})$ is the probability from state s_q to state s_p conditioned on our algorithm of Section III and the link set Ξ_{pq}.

The outage probability for state s_q can be calculated by

$$A_{qq} = \left(1 - \mathrm{P}_{\text{Single}}^{\text{SR}}\right)^{Q_{\text{SR}}} \times \left(1 - \mathrm{P}_{\text{Single}}^{\text{RD}}\right)^{Q_{\text{RD}}}. \tag{27}$$

The steady-state probabilities of $\boldsymbol{\pi} = [\pi_1, \ldots, \pi_{N_{\text{state}}}]^T \in \mathbb{R}^{N_{\text{state}} \times N_{\text{state}}}$ are calculated by

$$\boldsymbol{\pi} = (\mathbf{A} - \mathbf{I} + \mathbf{B})^{-1} \mathbf{b} \in \mathbb{R}^{N_{\text{state}}}, \tag{28}$$

where $\mathbf{I} \in \mathbb{R}^{N_{\text{state}} \times N_{\text{state}}}$ is the identity matrix, $\mathbf{b} = [1, \ldots, 1]^T \in \mathbb{R}^{N_{\text{state}}}$, and $\mathbf{B} = [\mathbf{b}, \ldots, \mathbf{b}] \in \mathbb{R}^{N_{\text{state}} \times N_{\text{state}}}$. Since the qth diagonal entry of $\mathbf{A}$ corresponds to the outage probability for state s_q, the theoretical bound on the outage probability is given by

$$\mathrm{P}_{\text{out}} = \mathrm{diag}(\mathbf{A})^T \boldsymbol{\pi}. \tag{29}$$

C. THEORETICAL THROUGHPUT

The theoretical throughput of the proposed scheme is represented by

$$\eta = \sum_{q=1}^{N_{\text{state}}} \pi_q \left(\sum_{p=1}^{N_q} A_{pq} \cdot \varepsilon_{pq} \right), \tag{30}$$

where ε_{pq} is the number of the different packets transmitted during the transmission mode from state q to state p, and N_q is the number of states reachable from state s_q.

D. THEORETICAL AVERAGE DELAY

According to [13], the average delay experience by the kth relay node is represented by

$$\mathbb{E}[D_k] = \frac{\mathbb{E}[\Psi_k]}{\eta_k}, \tag{31}$$

where $\mathbb{E}[\Psi_k]$ is the average number of packets stored at the kth relay node's buffer, and η_k is the average throughput at the kth relay node. The total average delay is calculated by the sum of the average delay at the source node $\mathbb{E}[D_S]$ and that at each relay node $\mathbb{E}[D_R]$, i.e.,

$$\mathbb{E}[D] = \mathbb{E}[D_S] + \mathbb{E}[D_R]. \tag{32}$$

Assuming that source information is saturated, the average delay at the source node is fixed at $\mathbb{E}[D_S] = 1$. In a two-hop network, we assume that the probability of selecting an SR link and that of selecting an RD link are the same, similar to [13]. Therefore, the average throughput of the network is given by $\eta/2$.

For $L = 2$ relay nodes, the throughput averaged over all the two relay nodes is given by

$$\eta_R = \frac{\eta}{2^2}, \tag{33}$$

and the queuing length averaged over all the two relay nodes is expressed as

$$\mathbb{E}[\Psi_R] = \frac{1}{2} \sum_{k=1}^{N_{\text{state}}} \pi_k \nu_k, \tag{34}$$

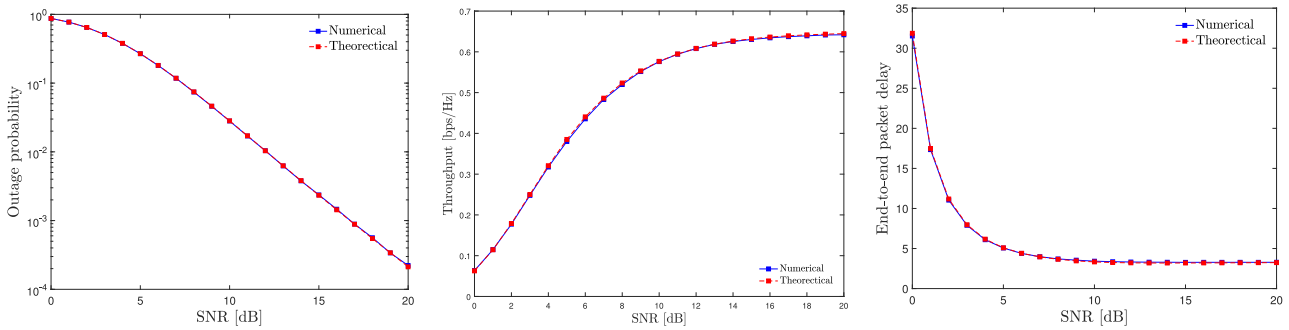

FIGURE 4. The numerical and theoretical results of the proposed scheme with the system parameters of $(K, L, \zeta_k) = (2, 2, 1)$; (a) the outage probability (b) the throughput and (c) the average delay.

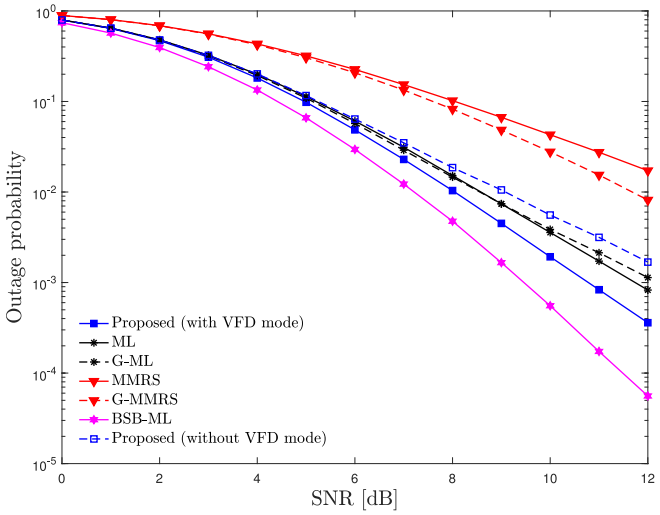

FIGURE 5. Outage probabilities of the proposed scheme (with and without the VFD mode), ML, G-ML, MMRS, G-MMRS and BSB-ML schemes with system parameters $(K, L) = (3, 3)$ and target number of packets $\zeta_k = 2$.

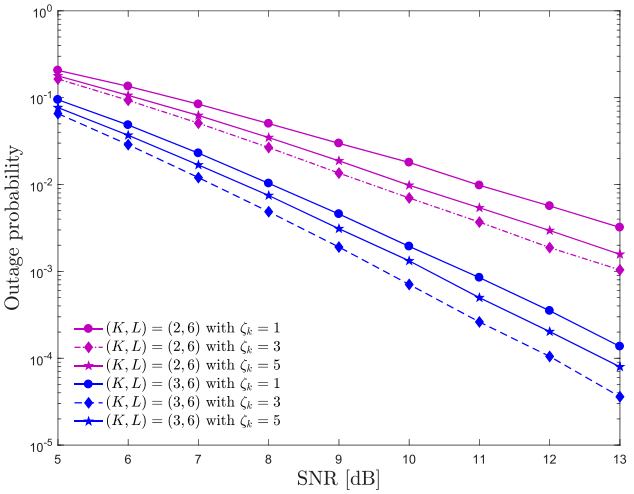

FIGURE 6. Outage probabilities of the proposed scheme with system parameters $(K, L) = (2, 6)$ and $(3, 6)$ and target number of packets $\zeta_k = 1$, 3, and 5.

where ν_i is the number of different packets stored at the relay nodes in state s_i. Then, the delay averaged over all the two relay nodes is given by

$$\mathbb{E}[D_R] = \frac{\mathbb{E}[\Psi_R]}{\eta_R} = \frac{2}{\eta} \sum_{k=1}^{N_{\text{state}}} \pi_k \nu_k. \tag{35}$$

Finally, the average delay of the network is formulated as

$$\mathbb{E}[D] = 1 + \frac{2}{\eta} \sum_{k=1}^{N_{\text{state}}} \pi_k \nu_k. \tag{36}$$

V. SIMULATION RESULTS

In this section, we provide our simulation results to show the proposed scheme's achievable performance. The performance is compared with the existing benchmark schemes, i.e., ML, G-ML, MMRS, G-MMRS, and BSB-ML [22]. The target rate of each node is fixed at $r_0 = 1$ bps/Hz. The initial buffer state of each relay node is set to be empty, and a sufficient number of packets are transmitted in each Monte Carlo simulation. Also, we considered the symmetric channel scenario of $\gamma_{\text{SR}} = \gamma_{\text{RD}}$.

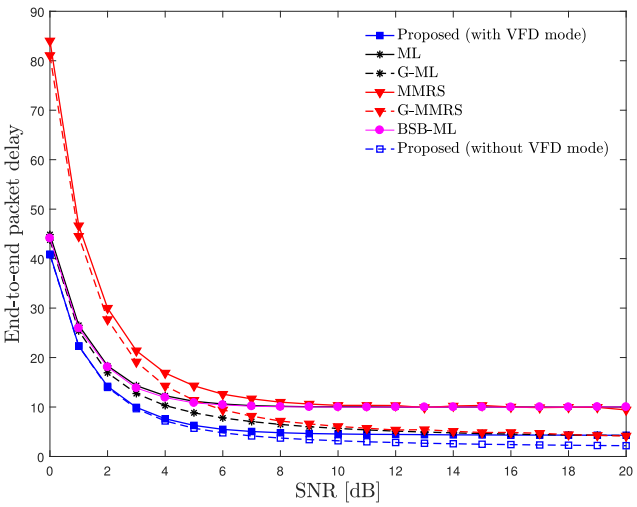

FIGURE 7. Average delay of the proposed scheme (with and without the VFD mode), ML, G-ML, MMRS, G-MMRS and BSB-ML schemes, with system parameters $(K, L) = (3, 3)$.

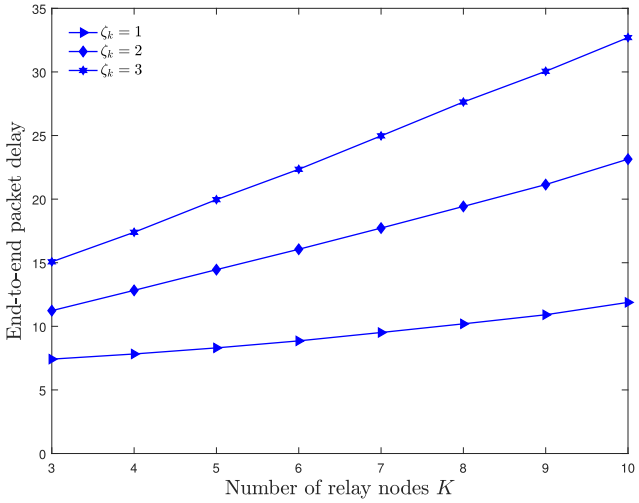

(a)

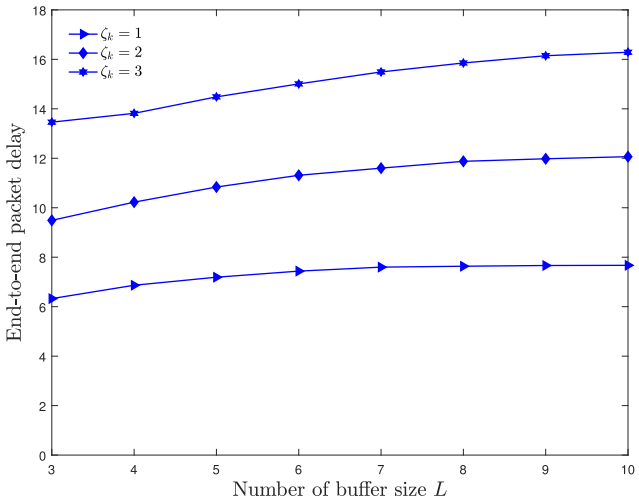

(b)

FIGURE 8. Average delay of the proposed scheme with the target number of packets $\zeta_k = 1$, 2, and 3; (a) $K = 3$ and (b) $L = 6$.

To validate our system model, in Fig. 4(a), we plotted the numerical and the theoretical curves of the proposed scheme for system parameters $(K, L, \zeta_k) = (2, 2, 1)$. Observe in Figs. 4(a), 4(b), and 4(c) that the numerical curves of the outage probability, the throughput, and the average delay curves coincided with the theoretical ones.

Next, Fig. 5 shows the outage probability of the proposed scheme with and without the VFD mode, and the five benchmarks, where we have used the system parameters $(K, L) = (3, 3)$ and the target number of packets was set to $\zeta_k = 2$. As shown in Fig. 5, the BSB-ML scheme exhibited a lower outage probability than the proposed scheme with the VFD mode, since the proposed scheme is focused more on high throughput and low average delay. Nevertheless, the proposed scheme with the VFD mode achieved the lowest outage probability of the remaining four schemes, owing to our adaptive multi-mode selection.

As shown in Fig. 6, we investigated the effect of target size ζ_k on the outage probability, considering the system

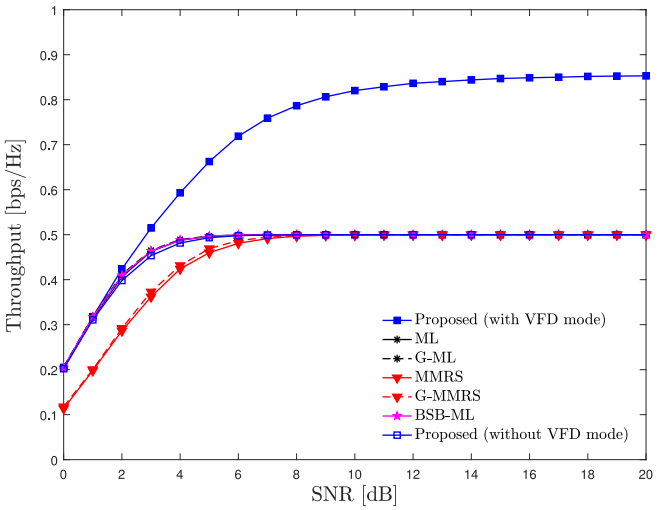

FIGURE 9. Average throughput of the proposed scheme (with and without the VFD mode), ML, G-ML, MMRS, and G-MMRS benchmarks shown for comparison, with system parameters $(K, L) = (6, 6)$.

parameters $(K, L) = (2, 6)$ and $(3, 6)$. The target number of packets was taken to be $\zeta_k = 1$, 3, and 5, while the average SNR was varied from $\gamma_t = 5$ dB to 13 dB. In each scenario for K, the proposed scheme with target value $\zeta_k = 3$ achieved the best performance. This may be because the detrimental states of both empty and full buffers were successfully avoided.

Fig. 7 shows the average delay of the proposed scheme (with and without the VFD mode) with the target number of packets $\zeta_k = 1$, which is compared with the five benchmark schemes. The system parameters were taken to be $(K, L) = (3, 3)$. Also, the average SNR was varied from $\gamma_t = 0$ dB to 20 dB. As a result, the proposed scheme without the VFD mode outperformed the five benchmark schemes. Moreover, the proposed scheme with the VFD mode can also provide lower average delay than the five benchmark schemes in the low SNR region of approximately $\gamma_t \leq 12$ dB. Furthermore, with the increase of the average SNR, the proposed scheme's average delay converged to a specific value, the same one as the G-ML and G-MMSE schemes.

To obtain further insight, in Fig. 8, we investigated the effects of the target number of packets ζ_k on the average delay, where the target number of packets was taken to be $\zeta_k = 1$, 2, and 3 while maintaining the SNR fixed at $\gamma_t = 5$ dB. Fig. 8(a) shows the results with the buffer size L varying and the number of relay nodes fixed at $K = 3$, whereas Fig. 8(b) shows those with the number of relay nodes K varying and the buffer size fixed at $L = 6$. Observe in Figs. 8(a) and 8(b) that the proposed scheme with target number $\zeta_k = 1$ achieved the lowest average delay. This is because the total number of packets stored in the buffers was kept low with $\zeta_k = 1$.

Next, the achievable average throughput was investigated. Fig. 9 compared the average throughput between the proposed scheme (with and without the VFD mode), the ML, G-ML, MMRS, G-MMRS, and BSB-ML benchmark schemes,

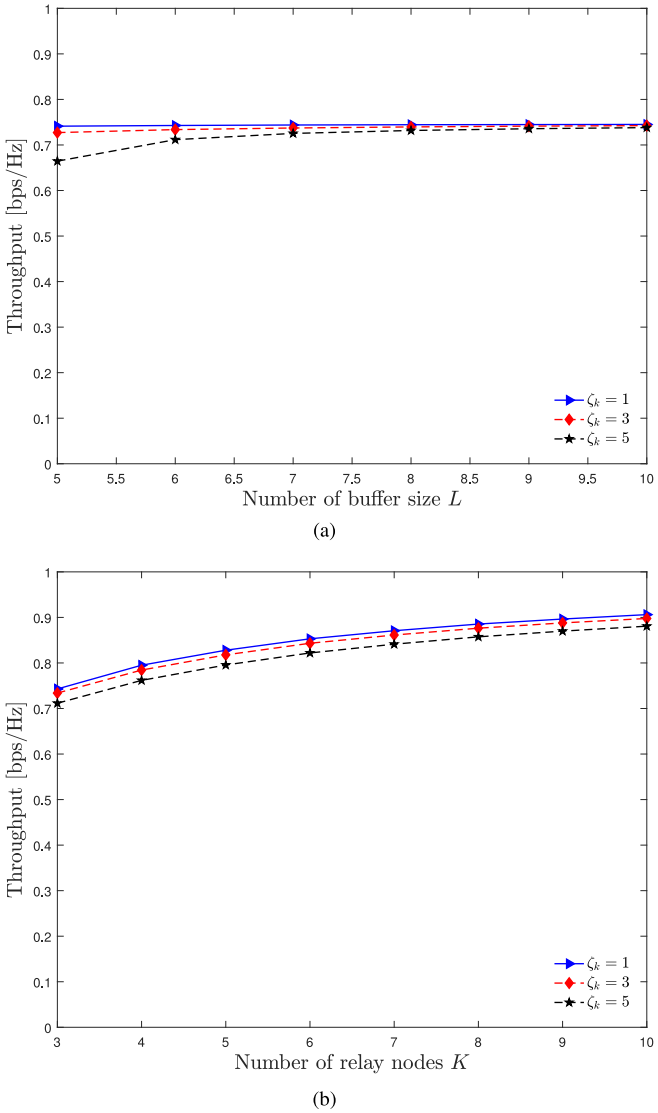

FIGURE 10. Throughput of the proposed scheme with the target number of packets taken to be $\zeta_k = 1$, 2, and 3; (a) $K = 3$, and (b) $L = 6$.

considering the system parameters of $(K, L) = (6, 6)$ and the target number of packets fixed at $\zeta_k = 1$. As shown in Fig. 9, the proposed scheme with the VFD mode outperforms the five benchmark schemes over the entire SNR range, owing to the VFD mode included in the proposed scheme. Also, the proposed scheme without the VFD mode exhibited an average throughput similar to that of the ML scheme.

In Fig. 10, the effects of ζ_k on the achievable average throughput were investigated for the SNR of 20 dB. The other system parameters used in Figs. 10(a) and 10(b) were the same as those of Figs. 8(a) and 8(b), respectively. In Figs. 10(a) and 10(b), it was found that the proposed scheme with $\zeta_k = 1$ achieved the highest throughput. This is expected from the theoretical average delay (36), which is proportional to the number of different packets stored in the buffers.

Finally, Fig. 11 shows the distribution of the transmission modes in the proposed scheme with the system parameters $(K, L) = (6, 10)$. The average SNR was varied from 0 dB

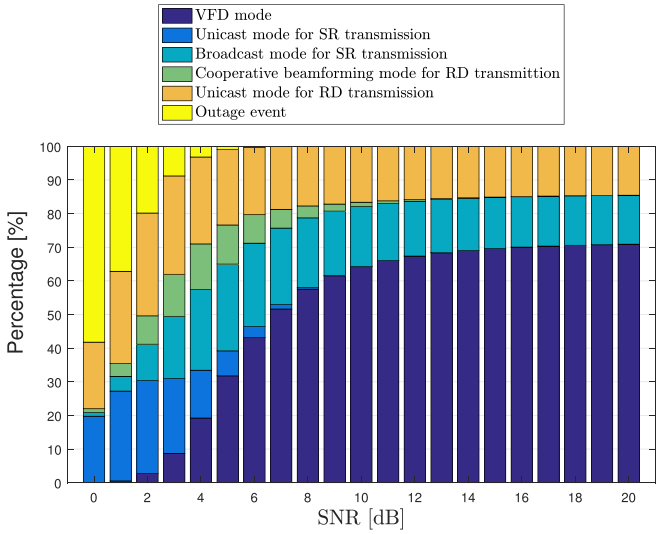

FIGURE 11. Distribution of the transmission modes in the proposed scheme with system parameters $(K, L) = (6, 10)$. Average SNR varies from 0 dB to 20 dB.

to 20 dB. As shown in Fig. 11, in the case of the lowest SNR value, 0 dB, the outage event dominated, followed by the unicast mode for SR and RD transmission, in that order. Upon increasing the SNR, the proportion of the VFD mode increased, contributing to a higher throughput. Also, it was observed that the VFD and the broadcast modes are dominant in the high SNR region (i.e., SNR $\geq$ 12 dB). This is because the VFD mode tended to be activated after a source packet was shared by relay nodes as a result of the activated broadcast mode.

VI. CONCLUSION

This paper proposed the buffer-aided relay selection scheme capable of adaptively selecting four HD transmission modes and a single VFD transmission mode. More specially, in the VFD mode, the detrimental effects of IRI are eliminated with the aid of SIC, which is enabled owing to a common packet shared by multiple relay nodes. The theoretical outage probability, throughput, and average delay bounds were derived. Our numerical results demonstrated that the proposed scheme provides higher average throughput than the four benchmark HD schemes. Also, the proposed scheme achieves a lower outage probability with an acceptable average delay profile than the benchmark schemes.

REFERENCES

[1] A. Nosratinia, T. E. Hunter, and A. Hedayat, "Cooperative communication in wireless networks," *IEEE Commun. Mag.*, vol. 42, no. 10, pp. 74–80, Oct. 2004.

[2] S. Sugiura, S. X. Ng, L. Kong, S. Chen, and L. Hanzo, "Quasi-synchronous cooperative networks: A practical cooperative transmission protocol," *IEEE Veh. Technol. Mag.*, vol. 7, no. 4, pp. 66–76, Dec. 2012.

[3] N. Nomikos *et al.*, "A survey on buffer-aided relay selection," *IEEE Commun. Surveys Tuts.*, vol. 18, no. 2, pp. 1073–1097, 2nd Quart., 2016.

[4] N. Zlatanov, A. Ikhlef, T. Islam, and R. Schober, "Buffer-aided cooperative communications: Opportunities and challenges," *IEEE Commun. Mag.*, vol. 52, no. 4, pp. 146–153, Apr. 2014.

[5] N. B. Mehta, V. Sharma, and G. Bansal, "Performance analysis of a cooperative system with rateless codes and buffered relays," *IEEE Trans. Wireless Commun.*, vol. 10, no. 4, pp. 1069–1081, Apr. 2011.

[6] R. Wang, V. K. N. Lau, and H. Huang, "Opportunistic buffered decode-wait-and-forward (OBDWF) protocol for mobile wireless relay networks," *IEEE Trans. Wireless Commun.*, vol. 10, no. 4, pp. 1224–1231, Apr. 2011.

[7] A. Ikhlef, D. S. Michalopoulos, and R. Schober, "Max-max relay selection for relays with buffers," *IEEE Trans. Wireless Commun.*, vol. 11, no. 3, pp. 1124–1135, Mar. 2012.

[8] I. Krikidis, T. Charalambous, and J. S. Thompson, "Buffer-aided relay selection for cooperative diversity systems without delay constraints," *IEEE Trans. Wireless Commun.*, vol. 11, no. 5, pp. 1957–1967, May 2012.

[9] C. Dong, L.-L. Yang, and L. Hanzo, "Performance analysis of multihop-diversity-aided multihop links," *IEEE Trans. Veh. Technol.*, vol. 61, no. 6, pp. 2504–2516, Jul. 2012.

[10] N. Zlatanov, R. Schober, and P. Popovski, "Buffer-aided relaying with adaptive link selection," *IEEE J. Sel. Areas Commun.*, vol. 31, no. 8, pp. 1530–1542, Aug. 2013.

[11] H. Liu, P. Popovski, E. de Carvalho, and Y. Zhao, "Sum-rate optimization in a two-way relay network with buffering," *IEEE Commun. Lett.*, vol. 17, no. 1, pp. 95–98, Jan. 2013.

[12] T. Islam, A. Ikhlef, R. Schober, and V. K. Bhargava, "Diversity and delay analysis of buffer-aided BICM-OFDM relaying," *IEEE Trans. Wireless Commun.*, vol. 12, no. 11, pp. 5506–5519, Nov. 2013.

[13] Z. Tian, G. Chen, Y. Gong, Z. Chen, and J. A. Chambers, "Buffer-aided max-link relay selection in amplify-and-forward cooperative networks," *IEEE Trans. Veh. Technol.*, vol. 64, no. 2, pp. 553–565, Feb. 2015.

[14] D. Chen, L.-L. Yang, and L. Hanzo, "Multi-hop diversity aided multi-hop communications: A cumulative distribution function aware approach," *IEEE Trans. Commun.*, vol. 61, no. 11, pp. 4486–4499, Nov. 2013.

[15] C. Dong, L.-L. Yang, J. Zuo, S. X. Ng, and L. Hanzo, "Energy, delay, and outage analysis of a buffer-aided three-node network relying on opportunistic routing," *IEEE Trans. Commun.*, vol. 63, no. 3, pp. 667–682, Mar. 2015.

[16] S. Huang, J. Cai, and H. Zhang, "Relay selection for average throughput maximization in buffer-aided relay networks," in *Proc. IEEE Int. Conf. Commun. (ICC)*, London, U.K., 2015, pp. 1994–1998.

[17] S. Luo and K. C. Teh, "Buffer state based relay selection for buffer-aided cooperative relaying systems," *IEEE Trans. Wireless Commun.*, vol. 14, no. 10, pp. 5430–5439, Oct. 2015.

[18] M. Oiwa and S. Sugiura, "Reduced-packet-delay generalized buffer-aided relaying protocol: Simultaneous activation of multiple source-to-relay links," *IEEE Access*, vol. 4, pp. 3632–3646, 2016.

[19] R. Nakai, M. Oiwa, K. Lee, and S. Sugiura, "Generalized buffer-state-based relay selection with collaborative beamforming," *IEEE Trans. Veh. Technol.*, vol. 67, no. 2, pp. 1245–1257, Feb. 2018.

[20] N. Nomikos, T. Charalambous, D. Vouyioukas, G. K. Karagiannidis, and R. Wichman, "Hybrid NOMA/OMA with buffer-aided relay selection in cooperative networks," *IEEE J. Sel. Topics Signal Process.*, vol. 13, no. 3, pp. 524–537, Jun. 2019.

[21] D. Q. Qiao and M. C. Gursoy, "Buffer-aided relay systems under delay constraints: Potentials and challenges," *IEEE Commun. Mag.*, vol. 55, no. 9, pp. 168–174, Sep. 2017.

[22] B. R. Manoj, R. K. Mallik, and M. R. Bhatnagar, "Performance analysis of buffer-aided priority-based max-link relay selection in DF cooperative networks," *IEEE Trans. Commun.*, vol. 66, no. 7, pp. 2826–2839, Jul. 2018.

[23] B. R. Manoj, R. K. Mallik, and M. R. Bhatnagar, "Buffer-aided multi-hop DF cooperative networks: A state-clustering based approach," *IEEE Trans. Commun.*, vol. 64, no. 12, pp. 4997–5010, Dec. 2016.

[24] M. Oiwa, R. Nakai, and S. Sugiura, "Buffer-state-and-thresholding-based amplify-and-forward cooperative networks," *IEEE Wireless Commun. Lett.*, vol. 6, no. 5, pp. 674–677, Oct. 2017.

[25] R. Nakai and S. Sugiura, "Physical layer security in buffer-state-based max-ratio relay selection exploiting broadcasting with cooperative beamforming and jamming," *IEEE Trans. Inf. Forensics Security*, vol. 14, pp. 431–444, 2019.

[26] R. Zhang, R. Nakai, K. Sezaki, and S. Sugiura, "Generalized buffer-state-based relay selection in cooperative cognitive radio networks," *IEEE Access*, vol. 8, pp. 11644–11657, 2020.

[27] J. Kochi, R. Nakai, and S. Sugiura, "Performance evaluation of generalized buffer-state-based relay selection in NOMA-aided downlink," *IEEE Access*, vol. 7, pp. 173320–173328, 2019.

[28] J. Kochi, R. Nakai, and S. Sugiura, "Hybrid NOMA/OMA broadcasting-and-buffer-state-based relay selection," *IEEE Trans. Veh. Technol.*, vol. 70, no. 2, pp. 1618–1631, Feb. 2021.

[29] A. Sabharwal, P. Schniter, D. Guo, D. W. Bliss, S. Rangarajan, and R. Wichman, "In-band full-duplex wireless: Challenges and opportunities," *IEEE J. Sel. Areas Commun.*, vol. 32, no. 9, pp. 1637–1652, Sep. 2014.

[30] S. Hong *et al.*, "Applications of self-interference cancellation in 5G and beyond," *IEEE Commun. Mag.*, vol. 52, no. 2, pp. 114–121, Feb. 2014.

[31] B. Debaillie *et al.*, "Analog/RF solutions enabling compact full-duplex radios," *IEEE J. Sel. Areas Commun.*, vol. 32, no. 9, pp. 1662–1673, Sep. 2014.

[32] D. Korpi, L. Anttila, V. Syrjälä, and M. Valkama, "Widely linear digital self-interference cancellation in direct-conversion full-duplex transceiver," *IEEE J. Sel. Areas Commun.*, vol. 32, no. 9, pp. 1674–1687, Sep. 2014.

[33] I. Krikidis, H. A. Suraweera, P. J. Smith, and C. Yuen, "Full-duplex relay selection for amplify-and-forward cooperative networks," *IEEE Trans. Wireless Commun.*, vol. 11, no. 12, pp. 4381–4393, Dec. 2012.

[34] A. Ikhlef, J. Kim, and R. Schober, "Mimicking full-duplex relaying using half-duplex relays with buffers," *IEEE Trans. Veh. Technol.*, vol. 61, no. 7, pp. 3025–3037, Sep. 2012.

[35] M. Oiwa and S. Sugiura, "Generalized virtual full-duplex relaying protocol based on buffer-aided half-duplex relay nodes," in *Proc. IEEE Global Commun. Conf.*, Singapore, Dec. 2017, pp. 1–6.

[36] B. Manoj, R. K. Mallik, M. R. Bhatnagar, and S. Gautam, "Virtual full-duplex relaying in multi-hop DF cooperative networks using half-duplex relays with buffers," *IET Commun.*, vol. 13, no. 5, pp. 489–495, Mar. 2019.

[37] S. M. Kim and M. Bengtsson, "Virtual full-duplex buffer-aided relaying in the presence of inter-relay interference," *IEEE Trans. Wireless Commun.*, vol. 15, no. 4, pp. 2966–2980, Apr. 2016.

[38] T. Mishina, M. Oiwa, R. Nakai, and S. Sugiura, "Buffer-aided virtual full-duplex cooperative networks exploiting source-to-relay broadcast channels," in *Proc. IEEE Veh. Technol. Conf.*, Honolulu, HI, USA, Nov. 2019, pp. 1–5.

[39] A. K. Shukla, B. R. Manoj, and M. R. Bhatnagar, "Virtual full-duplex relaying in a buffer-aided multi-hop cooperative network," in *Proc. Int. Conf. Signal Process. Commun. (SPCOM)*, Bangalore, India, 2020, pp. 1–5.

[40] N. Nomikos, T. Charalambous, N. Pappas, D. Vouyioukas, and R. Wichman, "LoLa4SOR: Leveraging successive transmissions for low-latency buffer-aided opportunistic relay networks," *IEEE Open J. Commun. Soc.*, vol. 2, pp. 1041–1054, 2021.

[41] R. Simoni, V. Jamali, N. Zlatanov, R. Schober, L. Pierucci, and R. Fantacci, "Buffer-aided diamond relay network with block fading and inter-relay interference," *IEEE Trans. Wireless Commun.*, vol. 15, no. 11, pp. 7357–7372, Nov. 2016.

[42] D. Qiao, "Fixed versus selective scheduling for buffer-aided diamond relay systems under statistical delay constraints," *IEEE Trans. Commun.*, vol. 65, no. 7, pp. 2838–2851, Jul. 2017.

[43] N. Nomikos, T. Charalambous, D. Vouyioukas, R. Wichman, and G. K. Karagiannidis, "Integrating broadcasting and NOMA in full-duplex buffer-aided opportunistic relay networks," *IEEE Trans. Veh. Technol.*, vol. 69, no. 8, pp. 9157–9162, Aug. 2020.

[44] N. Nomikos, T. Charalambous, D. Vouyioukas, and G. K. Karagiannidis, "When buffer-aided relaying meets full duplex and NOMA," *IEEE Wireless Commun.*, vol. 28, no. 1, pp. 68–73, Feb. 2021.

[45] G. Sriruthchataboon, J. Kochi, and S. Sugiura, "Hybrid buffer-aided relay selection based on half-duplex and virtual full-duplex transmission," in *Proc. IEEE Global Commun. Conf.*, Dec. 2021, pp. 1–6. [Online]. Available: http://dx.doi.org/10.36227/techrxiv.15086499.v1

[46] T. Islam, D. S. Michalopoulos, R. Schober, and V. K. Bhargava, "Buffer-aided relaying with outdated CSI," *IEEE Trans. Wireless Commun.*, vol. 15, no. 3, pp. 1979–1997, Mar. 2016.

[47] N. Nomikos, T. Charalambous, D. Vouyioukas, and G. K. Karagiannidis, "Low-complexity buffer-aided link selection with outdated CSI and feedback errors," *IEEE Trans. Commun.*, vol. 66, no. 8, pp. 3694–3706, Aug. 2018.

[48] V. Jamali, N. Zlatanov, and R. Schober, "Cooperative wireless backhauling," in *Proc. Int. ITG Conf. Syst. Commun. Coding (SCC)*, Hamburg, Germany, Feb. 2017, pp. 1–6.
[49] V. Jamali, N. Zlatanov, and R. Schober, "Bidirectional buffer-aided relay networks with fixed rate transmission—Part I: Delay-unconstrained case," *IEEE Trans. Wireless Commun.*, vol. 14, no. 3, pp. 1323–1338, Mar. 2015.
[50] V. Jamali, N. Zlatanov, and R. Schober, "Bidirectional buffer-aided relay networks with fixed rate transmission—Part II: Delay-constrained case," *IEEE Trans. Wireless Commun.*, vol. 14, no. 3, pp. 1339–1355, Mar. 2015.
[51] S.-R. Lee, S.-H. Moon, H.-B. Kong, and I. Lee, "Optimal beamforming schemes and its capacity behavior for downlink distributed antenna systems," *IEEE Trans. Wireless Commun.*, vol. 12, no. 6, pp. 2578–2587, Jun. 2013.

GAN SRIRUTCHATABOON received the B.E. degree in computer engineering from Bangkok University, Thailand, in 2005, and the M.E. degree in electrical engineering from Chulalongkorn University, Thailand, in 2015. He is currently pursuing the Ph.D. degree with the Institute of Industrial Science, The University of Tokyo, Tokyo, Japan. His research interest is in full-duplex communications.

JUN KOCHI received the B.E. degree in computer and information sciences from the Tokyo University of Agriculture and Technology, Koganei, Japan, in 2019, where he is currently pursuing postgraduate degree. His research interest is in non-orthogonal multiple access.

SHINYA SUGIURA (Senior Member, IEEE) received the B.S. and M.S. degrees in aeronautics and astronautics from Kyoto University, Kyoto, Japan, in 2002 and 2004, respectively, and the Ph.D. degree in electronics and electrical engineering from the University of Southampton, Southampton, U.K., in 2010.

From 2004 to 2012, he was a Research Scientist with Toyota Central Research and Development Laboratories, Inc., Aichi, Japan. From 2013 to 2018, he was an Associate Professor with the Department of Computer and Information Sciences, Tokyo University of Agriculture and Technology, Tokyo, Japan. Since 2018, he has been an Associate Professor with the Institute of Industrial Science, The University of Tokyo, Tokyo, where he heads the Wireless Communications Research Group. He authored or coauthored over 80 IEEE journal papers. His research has covered a range of areas in wireless communications, networking, signal processing, and antenna technology.

Dr. Sugiura was a recipient of numerous awards, including the Fifth Yasuharu Suematsu Award in 2019, the 33rd Telecom System Technology Award (Honorable Mention) from the Telecommunications Advancement Foundation in 2018, the Sixth RIEC Award from the Foundation for the Promotion of Electrical Communication in 2016, the Young Scientists' Prize by the Minister of Education, Culture, Sports, Science and Technology of Japan in 2016, the 14th Funai Information Technology Award (First Prize) from the Funai Foundation in 2015, the 28th Telecom System Technology Award from the Telecommunications Advancement Foundation in 2013, the Sixth IEEE Communications Society Asia–Pacific Outstanding Young Researcher Award in 2011, the 13th Ericsson Young Scientist Award in 2011, and the 2008 IEEE Antennas and Propagation Society Japan Chapter Young Engineer Award. He was also certified as an Exemplary Reviewer of IEEE COMMUNICATIONS LETTERS in 2013 and 2014, and IEEE TRANSACTIONS ON COMMUNICATIONS in 2018. He is currently serving as an Editor for IEEE WIRELESS COMMUNICATIONS LETTERS.